

# MR Imaging, targeting and characterization of pulmonary fibrosis using intra-tracheal administration of Gadolinium based nanoparticles

Nawal Tassali<sup>1</sup>, Andrea Bianchi<sup>1</sup>, François Lux<sup>2</sup>, Gerard Raffard<sup>1</sup>, Stéphane Sanchez<sup>1</sup>, Olivier Tillement<sup>2</sup>, and Yannick Cremillieux<sup>1</sup>

<sup>1</sup>Centre de Résonance Magnétique des Systèmes Biologiques, CNRS UMR 5536, Université de Bordeaux, Bordeaux, France, <sup>2</sup>Institut Lumière Matière, CNRS UMR 5306, Université Claude Bernard, Domaine Scientifique de la Doua, Villeurbanne, France

**Introduction:** Idiopathic pulmonary fibrosis (IPF) is a devastating and lethal disease characterized by excessive fibroblast and extracellular matrix (ECM) proliferation, resulting among other things in the thickening of blood-air barrier. Early and sensitive diagnostic tools are essential to assess the efficiency of therapies and to increase the life expectancy of patients suffering from this lung pathology. Among all imaging modalities, MRI distinguishes itself with its ability of detecting subtle tissue changes, its non-invasiveness and the absence of radiation. We propose here a novel approach using a MRI sequence combined with intra-tracheally administered gadolinium-based contrast agents for imaging and characterizing lung fibrosis. In this study, we quantified the signal enhancement (SE), the contrast to noise ratio (CNR), the pharmacokinetics (PK), the diffusion and elimination time constants of Ultra-Small Rigid Particles (USRPs) contrast agent in control mice and in a bleomycin-induced mouse model of lung fibrosis using an ultra-short echo time (UTE) MRI sequence.

**Materials and Methods:** MRI protocol: BALB/c and C57BL/6 (n=21) mice were used throughout the study. Treated mice were administered bleomycin via the Oropharyngeal Aspiration route.<sup>1</sup> UTE-MRI sequence was used for the detection of fibrosis lung injury from day 1 up to day 60 after the last administration of bleomycin. At day 30, 50 µL of a 50 mM Gd-based contrast agent solution was intra-tracheally (i.t) administered in the lungs of all mice and MR Images were immediately acquired (from 15 minutes up to 4 hours). Images were acquired with a 7T Bruker spectrometer using a transmitter/receiver quadrature coil of 25mm inner diameter (Bruker, Ettlingen, D). For each mouse, 10 axial slices of 1 mm thickness covering the entire lung were acquired in freely-breathing animals using a 2D UTE sequence with the following parameters: 804 directions/ 256 points, 4 averages, TE of 369 µs, FOV of 3cm, TR of 140 ms and FA of 60°, for a total acquisition time of 7.5 minutes. MR image analysis and quantification: the SE was calculated on two regions of interest in the lungs and averaged over the different measured slices. The CNR was computed as the difference between the average signal in the fibrotic and healthy tissues, normalized to the noise. Following the procedure described in ref 2, the longitudinal relaxation time (T<sub>1</sub>) was computed from the SE measurements. The concentration of the contrast agent in the lung was then obtained using the formula  $C(t) = \frac{1}{r_1} \left[ \frac{1}{T_1(t)} - \frac{1}{T_1(0)} \right]$  assuming the longitudinal relaxivity r<sub>1</sub> of USRPs at 7T equal to 60 mM<sup>-1</sup>s<sup>-1</sup> and T<sub>1</sub>(0)=1.6 s for the lungs. The diffusion and elimination time constant values of the USRPs were obtained using the PK model of ref 2. Histological analyses using hematoxylin-eosin to assess the general morphology and picrosirius red to identify collagen fibers were performed on the lungs of a subgroup of animals at day 30. Statistical analysis of the PK, the SE and CNR measurements was performed using a Mann-Whitney test.

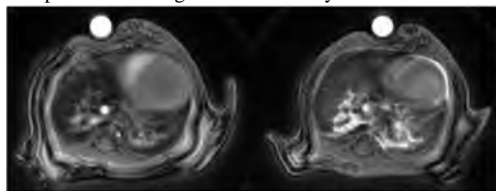


**Figure 1:** UTE-MRI lung images of bleomycin-treated mice at day 30. Left image was performed before the administration of contrast agent and right image was acquired 70 min after i.t administration of USRPs solution. A signal enhancement of 110% was obtained in fibrotic lesions.

**Figure 2:** Typical fits of the evolution of the concentration of the contrast agent in the lungs for a 50 mM USRPs solution for a given bleomycin-treated mouse at day 30 (in red) and for a given healthy mouse (in blue).

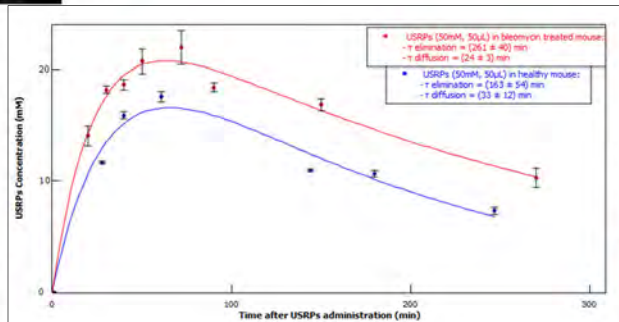
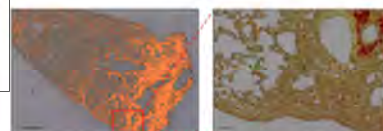


**Figure 3:** Typical picrosirius stained lung slices of bleomycin-treated animal. Orange areas correspond to collagen stained by picrosirius red. Magnification view x25 and scale bar of 200 µm for the left histological image. Magnification view x200 and scale bar of 100 µm for the right histological image.



**Results:** The onset of lung fibrosis was successfully monitored with MRI in all the bleomycin-treated mice up to 60 days after the end of the sensitization protocol. The bleomycin-induced lesions were essentially visualized in the central airways whereas distal regions of the lung had normal appearance in the UTE-MRI images. The i.t instillation of USRPs solution resulted in a SE larger than 120% in the area of fibrotic lesions (Fig.1). For comparison, in tissue where no fibrotic lesions were suspected in bleomycin-treated animals, the SE after USRPs instillation was inferior to 50%. In control animals, the SE in tissues was about 80%. Values measured in hyperintense and normal appearance regions in bleomycin-treated animals were significantly different (p<0.05). In all the bleomycin-treated mice, the increase of CNR in the identified fibrotic tissues 2 hours after the i.t of USRP solution showed almost twofold higher values (CNR about 40%) compared to the CNR before the administration of the particles (p<0.05). In bleomycin-treated mice, the average value of the diffusion time constant, corresponding to the passage of the nanoparticles from airspace to lung tissue and vascular compartment, was shorter compared to the healthy mice group. This difference was not statistically significant. The average elimination time constant of the USRPs from the lung tissue and vascular compartment was significantly longer as compared to healthy mice group. In C57BL/6 mice, the elimination time values were equal to 279.7 ± 34.5 min for treated mice and to 157.9 ± 13.5 min for healthy mice (Fig.2). The presence of lung fibrosis lesions was confirmed with histological analysis (Fig.3).

**Discussion and conclusion:** In this study, we showed that bleomycin-induced lung injury can be monitored using UTE-MRI and that large signal intensity enhancement and CNR in fibrotic lung tissue can be obtained when using intra-tracheal administration of non-targeting Gd-based contrast agents. Interestingly, the PK of contrast agents greatly varies between the healthy and the bleomycin-treated groups. The shortened diffusion time constant of the USRPs in the fibrosis animal group indicate a fast passage and accumulation of the contrast agent in disease regions of the lung. This observation might be related to this increase density of cellular component (ECM, fibroblast, proteoglycans) within fibrotic tissue. Proteoglycans are known to be hydrophilic and therefore could have a non-negligible affinity with the solution of contrast agent nanoparticles.<sup>3</sup> It can then be hypothesized that the ultrasmall contrast agent particles are rapidly diffusing from the airspaces to these fibrotic regions where they contribute to signal intensity enhancement. Similarly the longer elimination time constant observed in fibrotic animal group indicate a prolonged retention of the contrast agent within the disease lung tissue that can be related to the hampered access of the nanoparticles to the capillary blood vessels and their subsequent renal elimination. Further investigations are needed to validate the PK mechanisms and to understand the passive targeting and the behavior of the contrast agents within fibrotic tissues. However these results represent a clear demonstration of the potential of intra-tracheal administration of contrast agents and UTE lung MRI for a sensitive detection and characterization of the presence of fibrotic tissues.

**References:** <sup>1</sup>PLOS One, 2013, 8:63432 <sup>2</sup>MAGMA, 2014, 27:303-316 <sup>3</sup>Intensive Care Medicine, 2008, 34:610-618